INL/JOU-14-33448
PREPRINT

BWR Station Black Out: a RISMC Analysis Using Raven and RELAP5-3D

D. Mandelli, C. Smith, T. Riley,
J. Nielsen, A. Alfonsi, J. Cogliati,
C. Rabiti, J. Schroeder

January 2016

The INL is a
U.S. Department of Energy
National Laboratory
operated by
Battelle Energy Alliance

INL/ JOU-14-33448

BWR Station Black Out: a RISMC Analysis Using Raven and RELAP5-3D

**D. Mandelli, C. Smith, T. Riley,
J. Nielsen, A. Alfonsi, J. Cogliati,
C. Rabiti, J. Schroeder**

January 2016

**Idaho National Laboratory
Idaho Falls, Idaho 83415**

http://www.inl.gov

**Prepared for the
U.S. Department of Energy
Office of Nuclear Energy
Under DOE Idaho Operations Office
Contract DE-AC07-05ID14517**

BWR Station Black Out: a RISMC Analysis Using Raven and RELAP5-3D

D. Mandelli*, C. Smith, T. Riley, J. Nielsen, A. Alfonsi, J. Cogliati, C. Rabiti, J. Schroeder

Idaho National Laboratory

2525 North Fremont Ave

Idaho Falls, 83415 USA

Email: diego.mandelli@inl.gov

Number of pages: 15

Number of figures: 12

Number of tables: 6

ABSTRACT

The existing fleet of nuclear power plants is in the process of extending its lifetime and increasing the power generated from these plants via power uprates and improved operations. In order to evaluate the impact of these factors on the safety of the plant, the Risk-Informed Safety Margin Characterization (RISMC) project aims to provide insights to decision makers through a series of simulations of the plant dynamics for different initial conditions and accident scenarios. This paper presents a case study in order to show the capabilities of the RISMC methodology to assess impact of power uprate of a Boiling Water Reactor system during a Station Black-Out accident scenario. We employ a system simulator code, RELAP5-3D, coupled with RAVEN which perform the stochastic analysis. Our analysis is performed by: 1) sampling values from a set of parameters from the uncertainty space of interest, 2) simulating the system behavior for that specific set of parameter values and 3) analyzing the outcomes from the set of simulation runs.

Keywords: Dynamic PRA, Safety margin, SBO

I. INTRODUCTION

The Risk-Informed Safety Margin Characterization (RISMC) [1] Pathway, as part of the Light Water Sustainability (LWRS) Program [2], aims to develop simulation-based tools and methods to assess risks for existing Nuclear Power Plants (NPPs) in order to optimize safety. This Pathway, by developing new methods, is extending the Probabilistic Risk assessment (PRA) state-of-the-practice methods [3] which have been traditionally based on logic structures such as Event-Trees (ETs) and Fault-Trees (FTs) [4]. These static types of models mimic system response in an inductive and deductive way respectively, yet are restrictive in the ways they can represent spatial and temporal constructs. FTs are used to build logical event relationships between basic events (typically representing component failures) that affect branching conditions in the ET.

The ET structure follows a precise logic that is defined a priori by the user, i.e., the sequences of events in the ET are fixed and not interchangeable (in other words, they are part of a static model represented by a simple Boolean logic expression). As indicated in the historical accident in the nuclear industry, the timing of occurrence of such events can play a major role in the accident evolution. This timing information is not implicitly considered in an ET-FT structure; it is in fact only loosely considered in the definition of the basic events, e.g., DG recovery within 4 hours.

Both these issues (fixed logic structure, lack of timing considerations) preclude the ability to fully analyze possible accident evolution trajectories and, thus, also the possibility to evaluate importance of basic events in the overall core damage (CD) probability. This is one reason why the RISMC Pathway is employing state-of-the-art simulation based methodologies to evaluate accident evolution and the risk associated with these scenarios.

These issues are particularly relevant for RISMC where it is needed to evaluate the impact of plant changes such as power uprates and life extension on existing NPPs. From an ET-FT logic point of view, both power uprate and life extensions are not modeled, which further shows the limitations of this kind of methodologies for design and operational considerations.

In this paper we describe the RISMC approach and we will show this approach applied to a Boling Water Reactor (BWR) Station Black-Out (SBO) test case.

II. RISMC SIMULATION BASED APPROACH

The RISMC pathway uses the probabilistic margin approach to quantify impacts to reliability and safety. As part of the quantification, we use both probabilistic (via risk simulation) and mechanistic (via physics models) approaches, as represented in Fig. 1. Probabilistic analysis is represented by the risk analysis while mechanistic analysis is represented by the plant physics calculations. Safety margin and uncertainty quantification rely on plant physics (e.g., T-H and reactor kinetics) coupled with probabilistic risk simulation. The coupling takes place through the interchange of physical parameters (e.g., pressures and temperatures) and operational or accident scenarios.

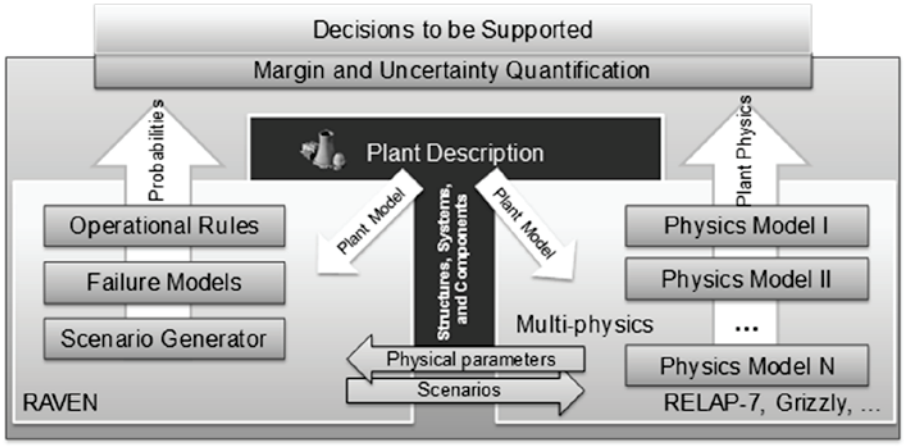

Fig. 1. Overview of the RISMC approach.

In Sec. I we have shown the main reasons behind the choice of moving from an ET-FT logic structure and employing directly system simulator codes to perform PRA analyses. A simulator code is, per se, a tool that can be represented as:

$$\frac{\partial \boldsymbol{\theta}(t)}{\partial t} = \boldsymbol{\mathcal{H}}(\boldsymbol{\theta}, \boldsymbol{p}, \boldsymbol{s}, t) \tag{1}$$

where:

- $\boldsymbol{\theta} = \boldsymbol{\theta}(t)$ represents the status of the system as function of time t, i.e., $\boldsymbol{\theta}(t)$ represents a single simulation
- $\boldsymbol{\mathcal{H}}$ is the actual simulator code that describes how $\boldsymbol{\theta}$ evolves in time

- $\boldsymbol{p} = \boldsymbol{p}(t)$ is the set of parameters internal to the simulator code (e.g., pipe friction coefficients, pump flow rate, reactor power)
- $\boldsymbol{s} = \boldsymbol{s}(t)$ represents the status of components and systems of the simulator (e.g., status of emergency core cooling system, AC system)

By using the RISMC approach, the PRA analysis is performed by:

1. Associating a probabilistic distribution function (pdf) to the set of parameters $\boldsymbol{p}$ and $\boldsymbol{s}$ (e.g., timing of events)
2. Performing sampling of the pdfs defined in Step 1
3. Performing a simulation run given $\boldsymbol{p}$ and $\boldsymbol{s}$ sampled in Step 2, i.e., solve Eq. (1)
4. Repeating Steps 2 and 3 N times and evaluate user defined stochastic parameters such CD probability (P_{CD}).

Strictly speaking, the sampling associated to the vector of parameters $\boldsymbol{p}$ is usually defined as uncertainty quantification while sampling the timing of events $\boldsymbol{s}$ is usually called PRA. In our applications, we include in the definition of PRA the sampling of both $\boldsymbol{p}$ and $\boldsymbol{s}$.

In order to perform PRA analyses of NPPs, the RISMC pathway is employing the RAVEN statistical framework [5] which is a recent add-on of the RAVEN package [6], that allows the user to perform generic statistical analysis. By statistical analysis we include: sampling of codes (e.g., Monte-Carlo [7] and Latin Hypercube Sampling [8], grid sampling, and Dynamic Event Tree [9]), generation of Reduced Order Models (ROMs) [10] (also known as surrogate models or emulators) and post-processing of the sampled data and generation of statistical parameters (e.g., mean, variance, covariance matrix).

Figure 2 shows an overview of the elements that comprise the RAVEN statistical framework:

- **Model**: it represents the pipeline between the input and output spaces. It is comprised of both interfaces for mechanistic codes (e.g., RELAP5-3D [11] and RELAP-7 [12]) and ROMs
- **Sampler**: it is the driver for any specific sampling strategy (e.g., Monte-Carlo [13], Latin Hypercube Sampling [14], Dynamic Event Tree [15])
- **Database**: the data storing entity
- **Post-processing**: module that performs statistical analyses and visualizes results

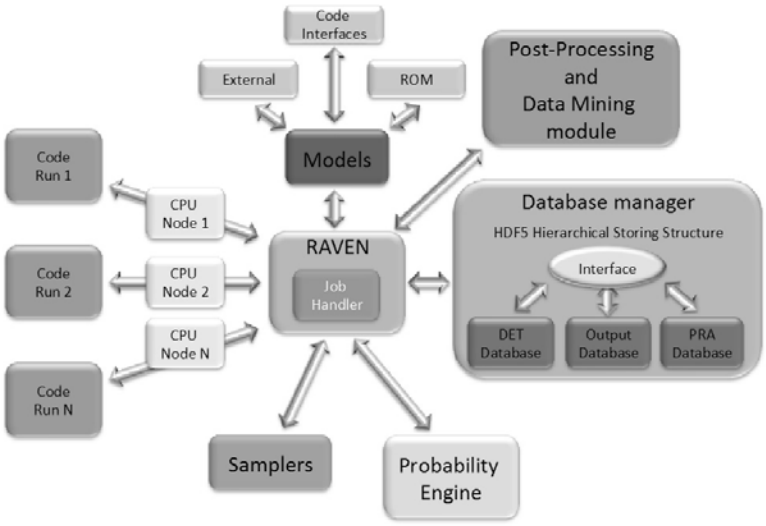

Fig. 2. Structure of RAVEN statistical framework components.

III. BWR SBO TEST CASE

The test case considered here for the RISMC approach is a BWR SBO initiating event. A description of the BWR model is shown in Sec. III.A while Sec. III.B describes in detail the accident scenario considered. Section III.C lists all the stochastic parameters that are sampled in the stochastic analysis and their associated distributions.

III.A. BWR Model

The system considered in this test case is a generic BWR power plant with a Mark I containment as shown in Fig. 3 (left). The main structures are the following [16]: Reactor Pressure Vessel (RPV), the pressurized vessel that contains the reactor core, and the primary containment. The primary containment includes: the Drywell (DW), the Pressure Suppression Pool (PSP), also known as wetwell, and the reactor circulation pumps. The PSP is a large torus shaped container that contains a large amount of water which is used as ultimate heat sink.

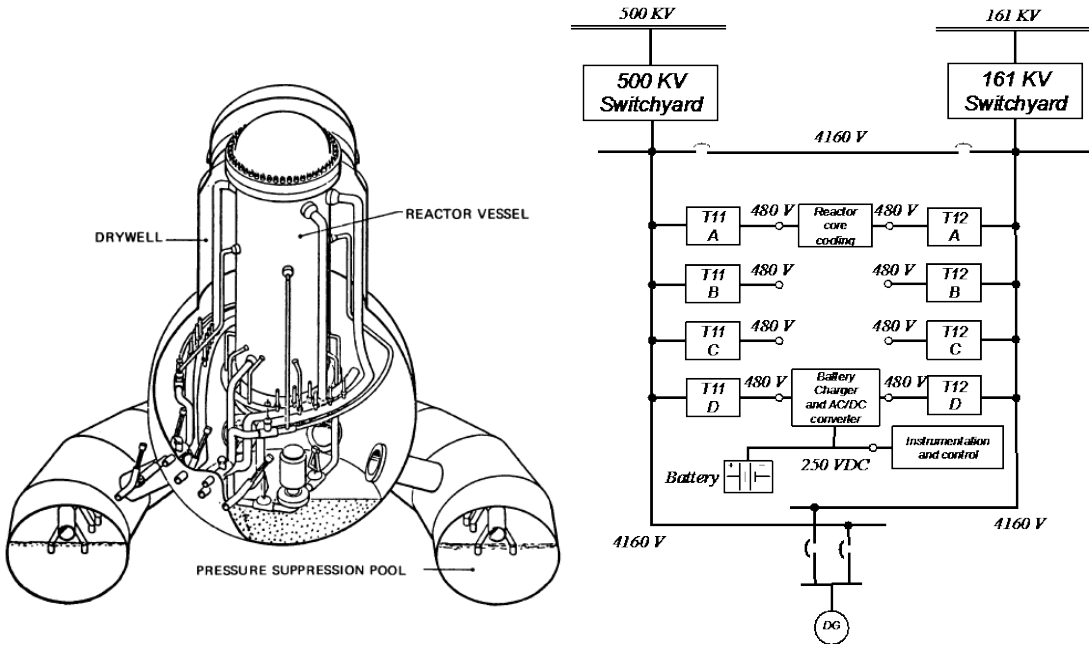

(a) (b)

Fig. 3. Overview of the BWR system with Mark I [17] (a) and the AC/DC power system schematics (b).

Three sources of core cooling water inventory are available:

1. Condensate Storage Tank (CST) that contains fresh water that can be used to cool the reactor core.
2. PSP water: PSP contains a large amount of fresh water that is used to provide the ultimate heat sink when AC power is lost.
3. Firewater (FW) system: water contained in the firewater system can be injected into the RPV when other water injection systems are disabled and when RPV is depressurized.

The high pressure RPV level control is provided by two systems: the Reactor Core Isolation Cooling (RCIC) and the High Pressure Coolant Injection (HPCI) systems. RCIC provides high-pressure injection of water from the CST to the RPV. Water flow from CST to the RPV is provided by a turbine driven pump that takes steam from the main steam line and discharges it to the PSP. Alternatively, the water source can be shifted from the CST to the PSP. HPCI is similar to RCIC but it allows greater water flow rates. Both RCIC and HPCI cannot be employed if the RPV is depressurized.

The RPV pressure control is provided by the Safety Relief Valves (SRVs) and the Automatic Depressurization System (ADS). SRVs are DC powered valves that control and limit the RPV pressure

within 900 and 1100 psi. The ADS consists of a separate set of relief valves that are employed to completely depressurize the RPV.

Several power systems are also included in the BWR model (see Fig. 3 right):

- Two independent power grids (500 KV and 161 KV) that are connected to the plant station thorough two independent switchyards.
- Diesel generators (DGs) which provide emergency AC power if power grid power is not available
- Battery systems: they provide DC power to instrumentation and control systems.

Complete loss of AC power disables the operability of all systems except: ADS, SRV, RCIC and HPCI (which requires only DC battery).

In an accident scenario, the set of emergency operating procedures requires the reactor operators to monitor not just the RPV but also the containment (both DW and PSP) thermo-hydraulic parameters (level, pressure and temperature). In this respect, a set of limit curves is provided to the reactor operator so that when they are crossed, the operators are required to activate the ADS system. These limit curves, also known as Heat Capacity Temperature Limits (HCTL), are shown in Fig. 4 and Fig. 5 for both PSP and DW respectively.

After ADS activation, not reactor core cooling is available unless AC power is recovered; alternatively, FW can be aligned to the RPV in order to provide core cooling.

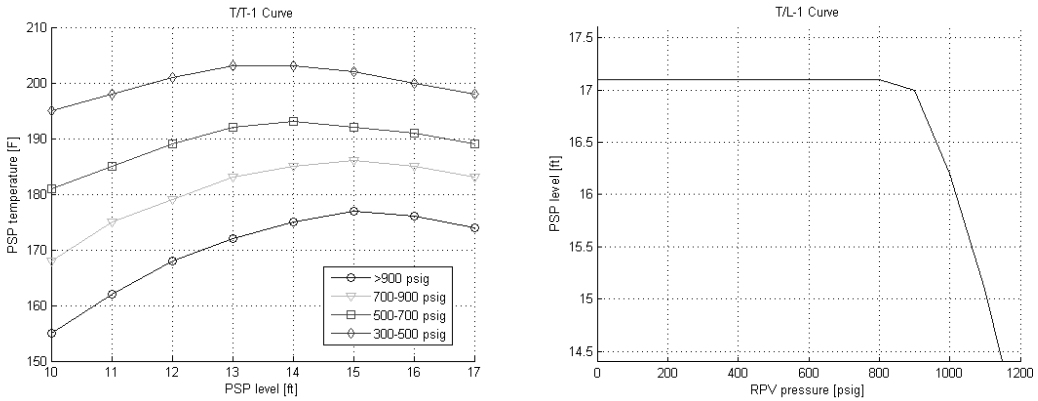

Fig. 4. HCTL curves for PSP.

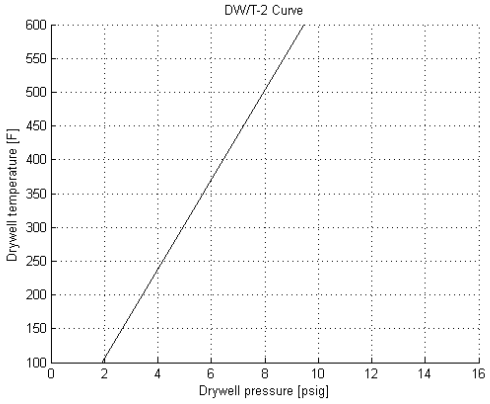

Fig. 5. HCTL curves for DW.

The BWR dynamic has been modeled using RELAP-5. The system nodalization is shown in Fig. 6 and it includes:

- RPV components such as the reactor core, down-comer, steam dome, jet-pump, SRVs, ADS
- Containment component such as PSP, drywell, recirculation pumps and CST
- External systems such as RCIC, HPCI, firewater

For the scope of this analysis we have decided to stop the simulation when one these three stopping conditions are met:

- Clad temperature reaches failure temperature
- AC power recovered
- Firewater available

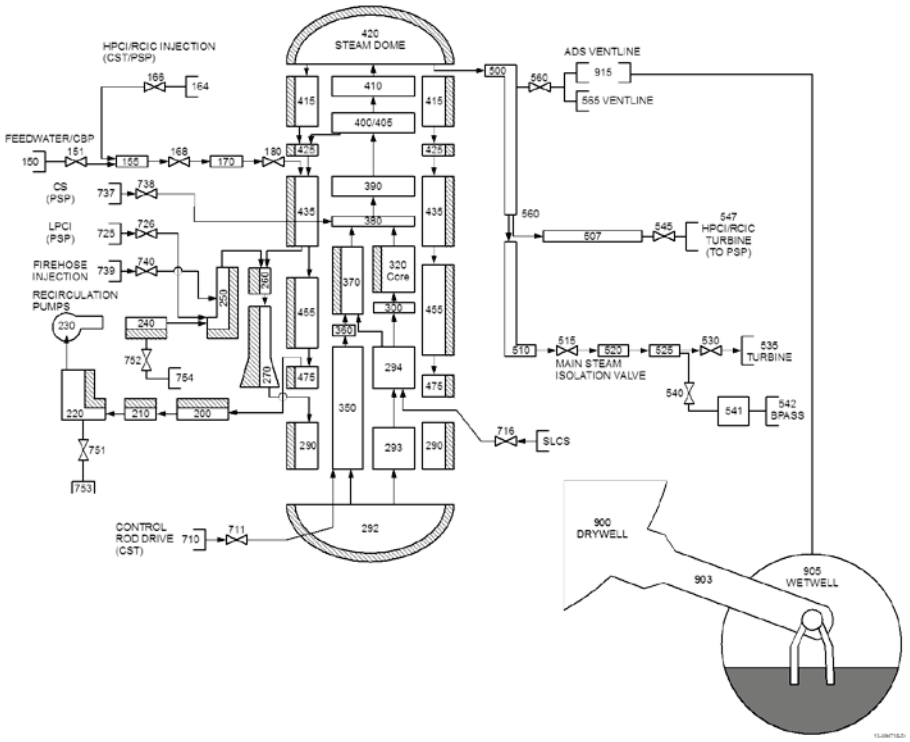

Fig. 6. RELAP5-3D nodalization of the BWR system.

III.B. SBO Scenario

The accident scenario under consideration is a loss of off-site power (LOOP) followed by loss of the DGs, i.e. SBO initiating event. In more detail, at time $t = 0$ the LOOP condition occurs due to external events (i.e., power grid related) which triggers the following actions:

- Operators successfully scram the reactor and put it in sub-critical conditions by fully inserting the control rods in the core
- Emergency DGs successfully start, i.e., AC power is available
- Core decay heat is removed from the RPV through the auxiliary core cooling system
- DC systems (i.e., batteries) are functional

At an uncertain time, SBO condition occurs: due to internal failure, the set of DGs fails. Thus removal of decay heat is impeded. Reactor operators start the SBO emergency operating procedures and perform:

- RPV level control using RCIC or HPCI
- RPV pressure control using SRVs
- Containment monitoring (both drywell and PSP)

At the same time, plant operators start recovery operations to bring back on-line the DGs while the recovery of the power grid is underway by the grid owner emergency staff.

Due to the limited life of the battery system and depending on the use of DC power, battery power can deplete. When this happens, all remaining control systems are offline causing the reactor core to heat until clad failure temperature is reached, i.e., CD.

If DC power is still available and one of these conditions are reached:

- Failure of both RCIC and HPCI
- HCTL limits reached
- Low RPV water level

then the reactor operators activate the ADS system in order to depressurize the RPV.

As an emergency action, when RPV pressure is below 100 psi plant staff can connect the firewater system to the RPV in order to cool the core and maintain an adequate water level. Such task is, however, hard to complete since physical connection between the firewater system and the RPV inlet has to made manually.

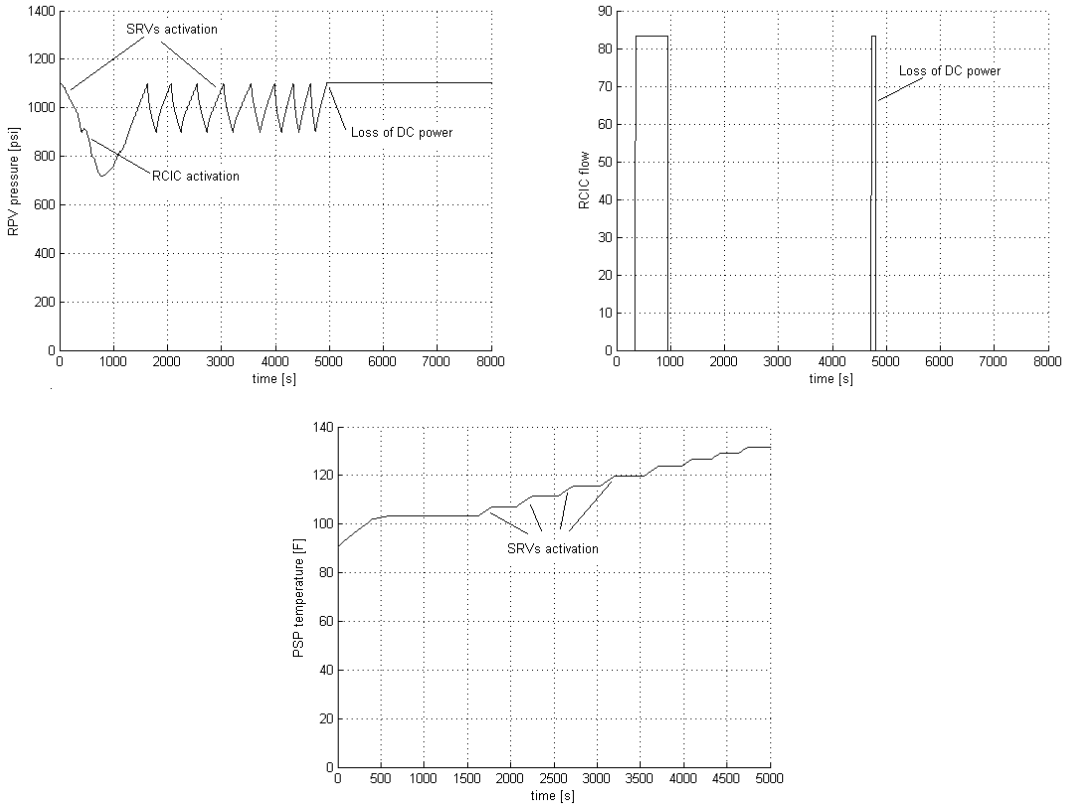

Fig. 7. Example of BWR SBO scenario.

When AC power is recovered, through successful re-start/repair of DGs or off-site power grid, auxiliary core cooling can be now employed to keep the reactor core cool.

An example of scenario is shown in Fig. 7:

- Following a failure to run of DGs, RPV pressure increases while RPV water level decreases. This triggers activation of both RCIC and SRVs.
- Cycling of SRV causes the PSP temperature to increase at each SRV activation
- RCIC activation causes RPV pressure to drop and RPV level to increase
- Loss of DC battery causes the impossibility to control both RPV level and pressure. While RPV level decreases, pressure is kept steady at around 1105 psi due to continue cycling of the RPV safety valves (automatic activation for RPV pressure greater than 1105 psi).

III.C. Stochastic Parameters

For this analysis we considered several uncertain parameters:

- *Failure time of DGs*: regarding the time at which the DGs fail to run we chose an exponential distribution with a value of lambda equal to 1.09 E-3 h^{-1}.
- *Recovery time of DGs*: Regarding time needed to recover the DGs, we used as a reference the NUREG/CR-6890 vol.1 [18]. This document uses a Weibull distribution[1] with $\alpha = 0.745$ and $\beta =$ 6.14 h (mean = 7.4 h and median = 3.8 h). Such distribution represents the pdf of repair of one of the two DGs (choosing the one easiest to repair).
- *Offsite AC power recovery*: For the time needed to recover the off-site power grid, we used as reference NUREG/CR-6890 vol.2 [19] (data collection was performed between 1986 and 2004). Given the four possible LOOP categories (plant centered, switchyard centered, grid related or weather related), severe/extreme events (such as earthquake) are assumed to be similar to these events found in the weather category (these are typically long-term types of recoveries). This category is represented with a lognormal distribution (from NUREG/CR-6890 [18]) with $\mu =$ 0.793 and $\sigma = 1.982$.
- *Battery life*: For the amount of DC power available, when AC power is not obtainable, we chose to limit battery life between 4 and 6 hours using a triangular distribution (see NUREG/CR-6890 vol.2 as reference [19]).
- *Battery failure time*: As basic event in the PRA model, the probability value associated with battery failure is equal to 1.4 E-5 for an expected life of 4 hours. We have assumed an exponential distribution for the battery failure time distribution. The value of λ for this distribution has been calculated by imposing that the CDF of this distribution ($1 - e^{-\lambda t}$) at 4 hours (i.e., the probability that battery fails within 4 hours is 1.4 E-5):

$$\int_0^4 \lambda\, e^{-\lambda t}\, dt = \left[1 - e^{-\lambda t}\right]_0^4 = 1.4 \text{ E-5}$$

This leads to a value of $\lambda = 3.5$ E-6/hr.

---

[1] Weibull distribution $pdf(x)$ is here defined as: $pdf(x) = \frac{\alpha}{\beta^{\alpha}} x^{\alpha-1} e^{-\left(\frac{x}{\beta}\right)^{\alpha}}$

- *SRVs fails open time*: the model used for this events has a probability value of 8.56 E-4.
- *Clad fail temperature*: Uncertainty in failure temperature for the clad is characterized by a triangular distribution [20] having:
    - Lower limit = 1800 F (982 C): PRA success criterion
    - Upper limit = 2600 F (1427 C): Urbanic-Heidrick transition temperature
    - Mode = 2200 F (1204 C): 10 CFR regulatory limit
- *RCIC fails to run*: Regarding the distribution of RCIC to fail to run, we assumed an exponential distribution with a rate of 4.43 E-3 per hour.
- *HPCI fails to run*: Identical distribution for RCIC fails to run distribution (see above)
- *Firewater flow rate*: The value of firewater flow rate is between 150 and 300 gpm [21]. For the scope of this report we also considered the possibility of very low firewater flow rates. Thus we assumed a triangular distribution defined in the interval [0,300] gpm with mode at 200 gpm.

Regarding the pdfs related to human related actions we looked into the SPAR-H [22] model. SPAR-H characterizes each operator action through eight parameters - for this study we focused on the two important factors: stress/stressors level and task complexity

These two parameters are used to compute the probability that such action will happen or not; these probability values are then inserted into the ETs that contain these events. However, from a simulation point of view we are not seeking if an action is performed but rather when such action is performed. Thus, we need a probability distribution function that defines the probability that such action will occur as function of time.

Since modeling of human actions is often performed using lognormal distributions [18], we chose such a distribution where its characters parameters (i.e., μ and σ) that are dependent on the two factors listed above (Stress/stressors level and Task complexity). We used Table 1 [23] to convert the three possible values of the two factors into numerical values for μ and σ.

TABLE I. Correspondence table between complexity and stress/stressor level and time values.

Complexity	μ (min)	Stress/stressors	σ (min)
High	45	Extreme	30
Moderate	15	High	15
Nominal	5	Nominal	5

For our specific case we modeled two human related actions as indicated below:

- *Battery repair time*: DC battery system restoration is performed by recovering batteries from nearby vehicles and connecting them to the plant DC system. We assumed that this task has high complexity with extreme stress/stressors level. This leads to $\mu = 45\ min$ and $\sigma = 15\ min$.
- *Firewater availability time*: The operations to align the firewater system to the RPV are considered a very complex operation. This time is measured after the ADS has been activated, i.e., after the RPV has been depressurized. Also for this case we assumed that this task has a high complexity with extreme stress/stressors level. This leads to $\mu = 45\ min$ and $\sigma = 30\ min$.

A summary of the distribution used is shown in Table 2.

TABLE II. Summary of the stochastic parameters and their associated distributions.

Stochastic variable*	Distribution type	*Distribution parameters*
Failure time of DGs (h)	Exponential	λ = *1.09 E-3*
Recovery time of DGs (h)	Weibull	$\alpha = 0.745$ *and* $\beta = 6.14$
Battery life (h)	Triangular	*(4, 5, 6)*
SRV 1 fails open time	Bernoulli	p = 8.56 E-4
Offsite AC power recovery (h)	Lognormal	$\mu = 0.793$ *and* $\sigma = 1.982$
Clad Fail temperature (F)	Triangular	*(1800, 2200, 2600)*
HPCI fails to run (h)	Exponential	λ = 4.43 E-3
RCIC fails to run (h)	Exponential	λ = 4.43 E-3
Battery failure time (h)	Exponential	λ = 3.5 E-6
Battery recovery time (min)	*Lognormal*	$\mu = 45$, $\sigma = 15$
Firewater availability time (min)	*Lognormal*	$\mu = 45$, $\sigma = 30$
Firewater flow rate (gpm)	Uniform	*(0, 200, 300)*

* - Parameters related to human operations are in *italic*

IV. SAFETY MARGIN ANALYSIS

This section shows some of the preliminary results regarding the effect of power uprates on SBO accident scenario. A higher value of thermal power generated in the core causes the following (see Fig. 8):

- Faster heating of the PSP and, thus, a reduction of the time interval between ADS activation time and loss of DG time, i.e., $T_{ADS}-T_{SBO}$
- A faster core temperature increase rate after ADS activation; thus leading to less time available to the plant staff to align the firewater

In summary, we expect that a power uprate reduces the time available to the plant staff to recover AC power and the time available to the plant staff to align FW. Scope of this section is to measure such reductions.

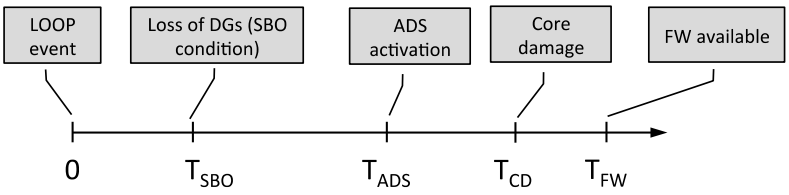

Fig. 8. Typical SBO sequence of events.

We performed an initial evaluation of the impact of power uprate by observing the PSP temperature increase rate as function of the thermal power generated by the core (see left image of Fig. 9). In particular, we looked at the time to reach the PSP temperature limits for different values of core power (ranging from 100% to 120%). These results are shown on the right image of Fig. 9. For this set of simulations we fixed T_{SBO} = 1 h and we, thus, measured $T_{ADS}-T_{SBO}$.

As expected, by increasing the core power, the time to reach the PSP heat capacity limits decrease. In the left graph in Fig. 9, the PSP temperature can be seen increasing in small steps as the SRVs open and close, and remaining relatively flat for a longer period of time whenever HPCI/RCIC activates and it is unnecessary to open the SRVs for a longer period of time. The sudden large increase in PSP temperature in each simulation is when the PSP heat capacity limit is reached and the ADS activates, dumping a huge amount of steam from the RPV into the PSP. Note that (Fig. 9 right), if reactor power is increased to 110% and 120%, the time to reach core HCTL limits decrease from 4.5 h (16300 s) to 3.9 h (14100 s) and 3.5 h (12400 s) respectively.

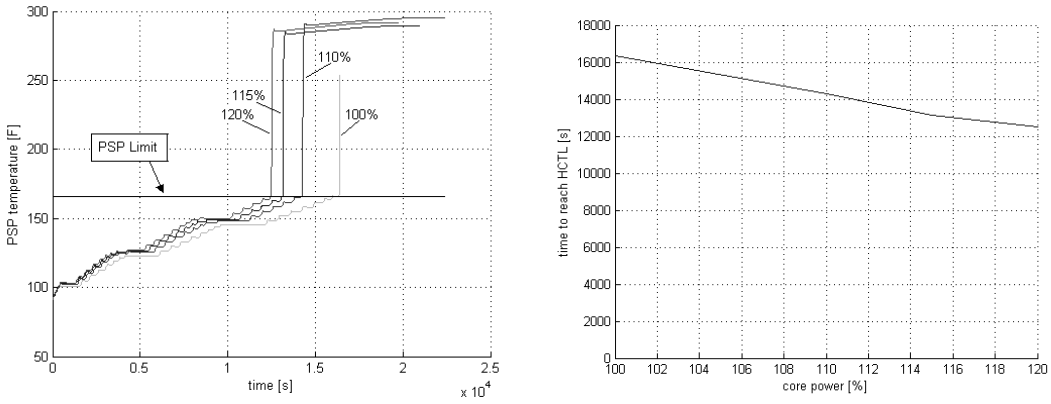

Fig. 9. Impact of reactor power uprate on time to reach PSP heat capacity limits HCTL.

We then considered the impact of power uprate for the following cases:

- Time to activate ADS vs. DG failure time (see Fig. 10 left)
- Time to reach CD vs. DG failure time (see Fig. 10 right)

From Fig. 10 note the following:

- We selected, for each power level (100%, 110% and 120%), a set of values for T_{SBO}. We then run a set of simulation runs and identified that time at which the reactor operators needs to activate the ADS. Compared to what is presented in Fig. 9, this analysis considered not just PSP temperature as indication to trigger ADS activation but all the curves shown in Fig. 4. In addition, AC power is not recovered and FW is never available.
- Fig. 10 (left) shows T_{SBO} (x axis) vs. T_{ADS}–T_{SBO} (y axis). By increasing T_{SBO}, we expect that the reactor operators are required to activate ADS much later. Again, a reactor power increase negatively affects ADS activation time.
- Fig. 10 (right) shows T_{SBO} (x axis) vs. T_{CD}–T_{SBO} (y axis). If AC power is available for a long time, the PSP HCTL limits are reached further in time. This allows reaching CD much later.

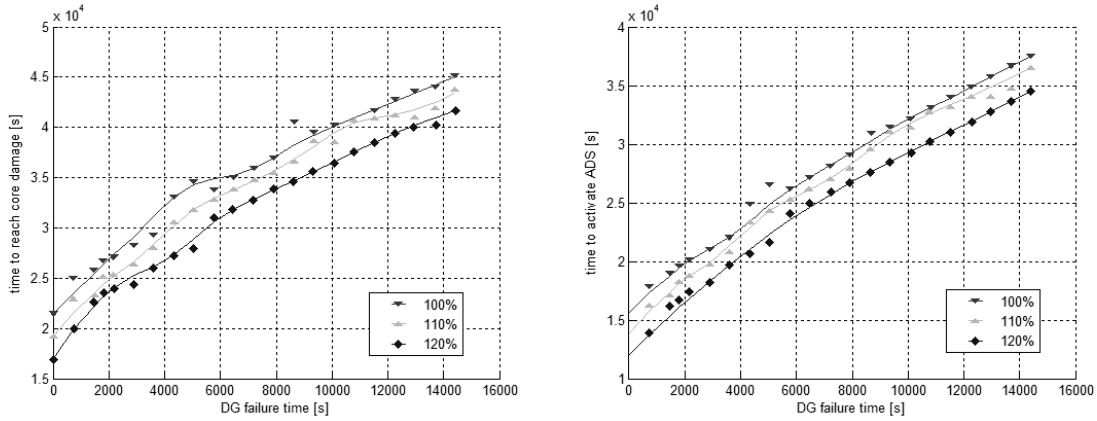

Fig. 10. Time to activate ADS vs. DG failure time (left) and time to reach core damage vs. DG failure time (right) curves for 100% (top curve), 110% (middle curve) and 120% power (bottom curve).

V. STOCHASTIC ANALYSIS

We performed two series of Latin Hypercube Sampling analysis for the two levels of reactor power (100% and 120%) using 10,000 samples for each case. The scope of this analysis is to evaluate how CD probability changes when reactor power is increased from 100% to 120%. We also performed this analysis by identifying importance of specific events by performing the following for each case:

1. Building an ET based logic structure that queries the following events: SRV status, DG, PG and FW recovery (see Fig. 11)
2. Associate each of the 10,000 simulations to a specific branch of the ET by querying the status of the SRV, PG, DG and FW components in the simulation run
3. Evaluate the probability and the outcome associated to each branch

A summary of the core damage probability for the cases is shown in Table 3: the probability value almost doubled for a 20% power increase. The summary of the branch probabilities represented in Fig. 11 is shown in Table 4. As expected, all branches that lead to CD have a probability increase while the ones leading to OK decrease. Branch 4, which is the driving branch for the CD event, doubles its probability value.

TABLE III. Core damage probability for two different power levels (100% and 120%).

Outcome	100%	120%
OK	0.990	0.980
CD	9.82 E-3	1.96 E-2

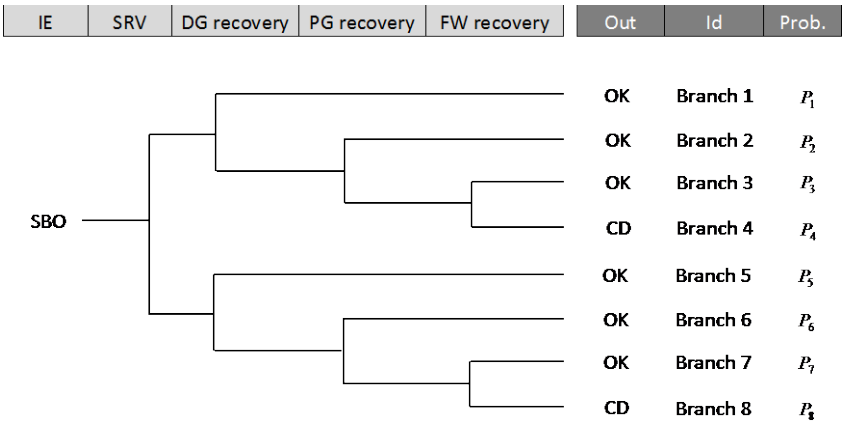

Fig. 11. Simplified ET logic structure for a BWR SBO.

TABLE IV. Branch probabilities associated to the ET shown in Fig. 11 for both cases (100% and 120% power).

Branch	Outcome	100%		120%		ΔP (%)
		Count	Probability	Count	Probability	
1	OK	3146	0.361	3238	0.353	-2.2
2	OK	4549	0.619	4440	0.617	-0.3
3	OK	847	0.00931	985	0.00926	-0.6
4	CD	557	0.00982	691	0.0196	+99
5	OK	333	7.32E-06	223	6.29E-06	-14
6	OK	254	1.53E-05	189	3.96E-06	-74
7	OK	251	5.92E-06	175	2.39E-06	-60
8	CD	63	2.12E-06	59	2.54E-06	+20

Regarding the FW flow rate, we were able to determine that a minimum value of 50 gpm is enough to assure an OK outcome. Note that branches 4 and 8 in Fig. 11 include also the simulations characterized by FW align before CD condition is met but with FW flow rate insufficient to keep the core cooled.

As second step in the analysis, we focused on the concept of limit surfaces [24]: the boundaries in the space of the sample parameters that separate failure from success. The advantage of limit surfaces is that they allow us to physically visualize how system performances are reduced due to, for example, a power uprate. By system performance, we mainly refer to both reduction in recovery timings (e.g., AC power recovery) and time reduction to perform steps in reactor operating procedures (e.g., time to reach HCTL).

For the scope of this article, we focused on a safety relevant case: DG failure time vs. DG recovery time as shown in Fig. 12. These limit surfaces are obtained using Support Vector Machines (SVM) based algorithms [25]. As expected the failure region (light grey) is expanding when reactor power is increased by 20%. This power increase on average reduces AC recovery time by about one hour.

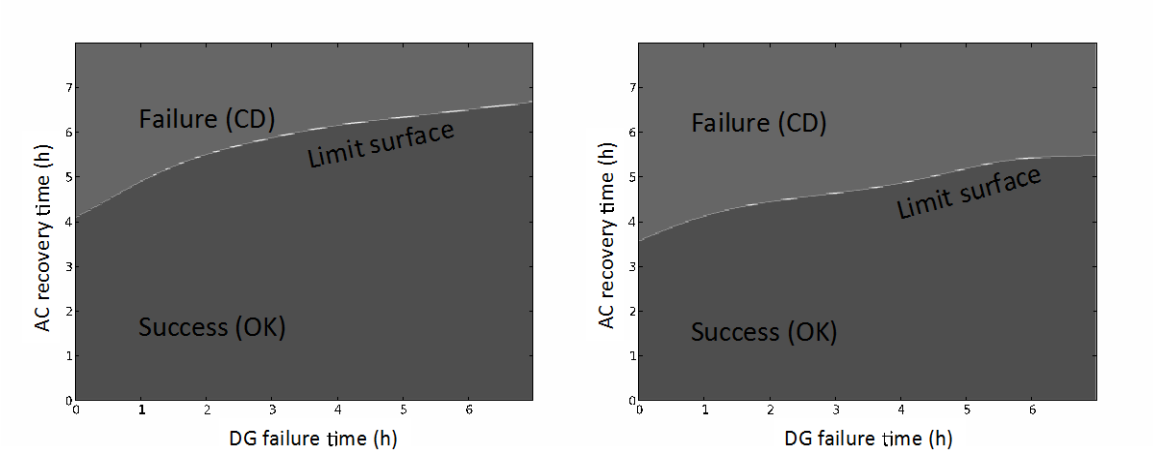

(a) (b)

Fig. 12. Limit surface obtained in a two dimensional space (DG failure time vs. AC recovery time) for two different power level: 100% (left) and 120% (right).

In addition to the analysis reported above, we evaluated the impact of auxiliary AC system generators as additional sources of AC power. The U.S. nuclear industry, as a measure after the Fukushima accident [26], developed a FLEX system to counterattack the risks associated with external events (e.g., earthquakes or flooding). Such a system employs portable AC and DC emergency generators located not only within the plant perimeter but also at strategic locations within the US borders in order to quickly supply affected NPPs with both AC and DC power.

For our case, we assumed a new distribution associated with the AC recovery time within the plant instead of the DG recovery time distribution. Since FLEX operations can be considered as human-related events, we followed the same approach described in Sec. III.C for human related events (see Table 1). We assumed that the AC recovery can be considered to be of moderate complexity and high levels of stress/stressors. Note that this model may not be indicative of any actual NPP FLEX strategies – for an actual FLEX evaluation, plant specific information would need to be considered. The new AC recovery distribution that replaces the DG recovery distribution is then a lognormal having a mean and a standard deviation values as follows:

- mean = 15.0
- standard deviation = 15.0

We then performed a new Latin Hypercube Sampling analysis in order to estimate the new CD probability value and the branch probabilities associated with the ET structure shown in Fig. 11. Results are

summarized in Table 5 and Table 6. Note from Table 5 a decrease in CD probability due to the fact that the new distribution has much lower mean value.

TABLE V. Core damage probability for two different test cases (120% with and without FLEX system).

Outcome	120% w/o FLEX	120% w/ FLEX
OK	0.981	0.995
CD	1.96 E-2	4.59 E-3

TABLE VI. Branch probabilities for two different test cases (120% with and without FLEX system).

Branch	Outcome	Probability (120%)		ΔP (%)
		w/o FLEX	w/ FLEX	
1	OK	0.353	0.505	43
2	OK	0.618	0.490	-21
3	OK	0.009258	3.49E-05	-100
4	CD	0.0196	0.00459	-77
5	OK	6.29E-06	2.87E-06	-54
6	OK	3.96E-06	1.79E-09	-100
7	OK	2.39E-06	6.77E-10	-100
8	CD	2.54E-06	1.09E-09	-100

VI. CONCLUSIONS

In this article we have shown the RISMC approach in order to evaluate the impact of power uprate on a BWR SBO accident scenario. We have employed RELAP5-3D as system simulator code and the RAVEN code to perform the accident sequence generation and statistical analysis. The BWR system, the system control logic and the accident scenario have been directly implemented in the RELAP5-3D input file. We evaluate the increase of CD probability of such power uprate and its decrease due to the implementation of FLEX system to provide emergency power to the plant. In particular, we have shown how the RISMC approach to perform PRA analyses can overcome limitations of classical ET-FT based methodologies and provide the user to a much larger amount of information such as time reduction for plant recovery strategies.

ACKNOWLEDGMENTS

This work was accomplished through the RISMC Pathway as part of the DOE Light Water Reactor Sustainability (LWRS) Program.

REFERENCES

1. C. Smith, C. Rabiti, and R. Martineau, "Risk Informed Safety Margins Characterization (RISMC) pathway technical program plan," Idaho National Laboratory Technical Report INL/EXT-11-22977 (2011).
2. DOE-NE Light Water Reactor Sustainability Program and EPRI Long-Term Operations Program – Joint Research and Development Plan, Revision 3, INL-EXT-12-24562 (2014).
3. U.S.NRC, NUREG 1150, "Severe accident risks: an assessment for five U.S. nuclear power plants," Division of Systems Research, Office of Nuclear Regulatory Research, U.S. Nuclear Regulatory Commission, Washington, DC (1990).
4. U.S.NRC, WASH 1400, "Reactor Safety Study - An Assessment of Accident Risks in U.S. Commercial Nuclear Power Plants," Division of Systems Research, Office of Nuclear Regulatory Research, U.S. Nuclear Regulatory Commission, Washington, DC (1975).
5. C. Rabiti, A. Alfonsi, D. Mandelli, J. Cogliati, R. Martinueau, C. Smith, "Deployment and overview of RAVEN capabilities for a probabilistic risk assessment demo for a PWR Station blackout," Idaho National Laboratory Technical Report INL/EXT-13-29510 (2013).
6. C. Rabiti, D. Mandelli, A. Alfonsi, J. Cogliati, and B. Kinoshita, "Mathematical framework for the analysis of dynamic stochastic systems with the raven code," in Proceedings of International Conference of mathematics and Computational Methods Applied to Nuclear Science and Engineering (M&C 2013), Sun Valley (Idaho) (2013).
7. E. Zio, M. Marseguerra, J. Devooght, and P. Labeau, "A concept paper on dynamic reliability via Monte Carlo simulation," in Mathematics and Computers in Simulation, 47, pp. 371-382, (1998).
8. J.C. Helton and F. J. Davis, "Latin hypercube sampling and the propagation of uncertainty in analyses of complex systems," Reliability Engineering & System Safety, 81-1 (2003).
9. A. Amendola and G. Reina, "Dylam-1, a software package for event sequence and consequence spectrum methodology," in EUR-924, CEC-JRC. ISPRA: Commission of the European Communities (1984).
10. N.V. Queipo, R.T. Haftka, W. Shyy, T. Goel, R. Vaidyanathan, P.K. Tucker, "Surrogate-based analysis and optimization," Progress in Aerospace Sciences, 41, pp. 1-28 (2005).

11. RELAP5 Code Development Team, “RELAP5-3D Code Manual”, Idaho National Laboratory Technical Report INEEL-EXT-98-00834 (2012).
12. A. David, R. Berry, D. Gaston, R. Martineau, J. Peterson, H. Zhan, H. Zhao, L. Zou, “RELAP-7 Level 2 milestone report: demonstration of a steady state single phase PWR simulation with RELAP-7,” Idaho National Laboratory Technical Report INL/EXT-12-25924 (2012).
13. A. Alfonsi, C. Rabiti, D. Mandelli, J. Cogliati, and R. Kinoshita, “Raven as a tool for dynamic probabilistic risk assessment: Software overview,” in Proceedings of International Conference of mathematics and Computational Methods Applied to Nuclear Science and Engineering (M&C 2013), Sun Valley (Idaho), (2013).
14. C. Rabiti, A. Alfonsi, D. Mandelli, J. Cogliati and R. Kinoshita, “Advanced probabilistic risk analysis using RAVEN and RELAP-7”, Idaho National Laboratory Technical Report INL/EXT-14-32491 (2014).
15. A. Alfonsi, C. Rabiti, D. Mandelli, J. Cogliati, and R. Kinoshita, “RAVEN: Dynamic event tree approach,” Idaho National Laboratory Technical Report INL/EXT-13-30332 (2013).
16. D. Mandelli, C. Smith, T. Riley, J. Schroeder, C. Rabiti, A. Alfonsi, J. Nielsen, D. Maljovec, B. Wang, and V. Pascucci, “Support and modeling for the boiling water reactor station black out case study using RELAP and RAVEN,” Idaho National Laboratory Technical Report INL/EXT-13-30203 (2013).
17. D. H. Cook, S. R. Greene, R. M. Harrington, S. A. Hodge, D. D. Yue, “NUREG/CR-2182, Vol 1, Station Blackout at Browns Ferry Unit One - Accident Sequence Analysis,” Prepared for the U.S. Nuclear Regulatory Commission Office of Nuclear Regulatory Research (1981).
18. S. Eide et al, “Reevaluation of station blackout risk at nuclear power plants”, U. S. Nuclear Regulatory Commission, NUREG/CR-6890 Vol. 1, Analysis of Loss of Offsite Power Events: 1986-2004 (2005).
19. S. Eide et al, “Reevaluation of station blackout risk at nuclear power plants”, U. S. Nuclear Regulatory Commission, NUREG/CR-6890 Vol. 2, Analysis of Station Blackout Risk (2005).
20. R. Sherry and J. Gabor, “Pilot Application of Risk Informed Safety Margins to Support Nuclear Plant Long Term Operation Decisions – Impacts on Safety Margins of Power Uprates for Loss of Main Feed-water Events”, EPRI. Palo Alto, CA, 1025291 (2012).

21. U.S.NRC, “NUREG/CR-7110 State-of-the-Art Reactor Consequence Analysis (SOARCA) Project Surry Integrate Analyses Report” Volume IV.
22. D. Gertman, H. Blackman, J. Marble, J. Byers and C. Smith, “NUREG/CR-6883: The SPAR-H Human Reliability Analysis Method”, Nuclear Regulatory Commission US-NRC (2005).
23. D. Mandelli, C. Smith, Z. Ma, T. Riley, J. Nielsen, A. Alfonsi, C. Rabiti, J. Cogliati, “Risk-Informed Safety Margin Characterization Methods: Development Work,” Idaho National Laboratory Technical Report INL/EXT-14-33191 (2014).
24. D. Mandelli and C. Smith, “Adaptive sampling using Support Vector Machines,” in Proceeding of American Nuclear Society (ANS), San Diego (CA), 107, pp. 736-738 (2012).
25. C. J. C. Burges, “A tutorial on Support Vector Machines for pattern recognition,” Data Mining and Knowledge Discovery, 2, pp. 121-167 (1998).
26. Institute of Nuclear Power Operations, “Special Report on the nuclear accident at the Fukushima Daiichi nuclear power station”, INPO report 11-005 (2011).